JOURNAL OF OPTOELECTRONICS AND ADVANCED MATERIALS Vol. 10, No. 4, April 2008, p. 744 - 749

Invited Paper

On the magnetic properties of $RFe_{11}TiH_x$ compounds

O. ISNARD*, M. GUILLOT[a]
Institut Néel, CNRS, associé à l'Université J. Fourier de Grenoble, avenue des martyrs, BP166, 38042 Grenoble, Cédex 9, France
[a]*Laboratoire des Champs Magnétiques Intenses, CNRS, avenue des martyrs, BP166, 38042 Grenoble, Cédex 9, France*

Hydrogen atoms insertion within the crystal structure of the $RFe_{11}Ti$ compounds induces a significant modification of the physical properties. This includes an anisotropic unit cell expansion as well as a large increase of the Curie temperature. Other magnetic properties such as the magnetocrystalline anisotropy are also affected by H insertion within the lattice. The magnetic phase diagram of the $TmFe_{11}TiH_x$ and $TbFe_{11}TiH_x$ compounds have been investigated by combining neutron diffraction, magnetic measurements as well as high magnetic field measurements. The competition between the magnetocrystalline anisotropy terms can lead to spin reorientation phenomena in $RFe_{11}TiH$ with some rare-earth whereas for some others like Tb the spin reorientation transitions observed in the $TbFe_{11}Ti$ compounds has disappeared. In the case of the Tm compound a uniaxial character is observed up to the Curie temperature.

(Received February 25, 2008; accepted April 2, 2008)

Keywords: Hard magnetic materials, Hydrogen, Magnetic phase diagram, Interstitial element, $RFe_{11}TiH_x$

1. Introduction

The $ThMn_{12}$ type compounds are among the richest intermetallic in transition metal [1,2]. The iron or cobalt containing isotype are of interest since they may exhibit high ordering temperature and large magnetization. Unfortunately the $ThMn_{12}$ structure type is not present in the R-Fe (R being a rare-earth element) binary phase diagram. Nevertheless this structure type is stabilized by a partial substitution of other elements like Ti, Mo, V, Cr… to Fe atoms thus leading to the following formula $RFe_{12-x}M_x$ [1,2]. Among this pseudo binary series the Ti containing phases have attracted interest since they are stabilized with a small amount of substitution leading to iron rich content [3,4]. They are considered as potential candidate for permanent magnet applications. From the fundamental point of view they are also very interesting since they can exhibit very complex magnetic phase diagram resulting from the possible competition of the anisotropy parameters of the rare-earth sublattice and the iron sublattice. That explains why some $RFe_{12-x}Ti_x$ have been widely studied [3-9]. More recently, the insertion of interstitial element like H, C or N within the $RFe_{12-x}Ti_x$ has also been performed leading to dramatic change of the magnetic properties [5,10-16]. Here, following our previous investigation [5,13,14], we will concentrate on the effect of hydrogen insertion on the structural and magnetic properties of the $RFe_{12-x}Ti_x$ with an emphasis on R=Tm and Tb.

2. Experimental

The samples used herein are the same as that used in our earlier studies [5,13,14]. The alloys have been obtained by melting the starting elements in a high frequency induction furnace equipped with a water cooled copper crucible. The homogeneity of the ingot was subsequently achieved by annealing at 950 °C for 10 days. The hydrogen insertion has been carried out under 20 bar of H_2 gas and thermal activation was needed to initiate the reaction. The amount of absorbed hydrogen estimated by gravimetric as well as volumetric method was about one H atom per $RFe_{11}Ti$ formula unit. Such estimation of this hydrogen content has been confirmed by neutron diffraction on several $RFe_{11}Ti$ isotype compound [15-17]. The structural parameters were derived from X-ray diffractometry. The X-ray patterns were recorded using a Guinier-Hägg focusing camera operated at Fe K_α radiation, with silicon as an internal standard. The lattice parameters have been refined taking into account 22 observed Bragg reflections. Thermomagnetic analysis of the sample being sealed in a silica tube to avoid oxidization or hydrogen release was performed using a Faraday type balance.

The Isothermal magnetization M *vs* H curves were carried out on magnetically aligned powder of the $RFe_{11}TiH_x$ samples was measured between 4.2 and 295 K in applied fields of zero to 23 T produced by a water-cooled Bitter magnet at the Laboratoire des Champs Magnétiques Intenses in Grenoble, France. All the samples were sieved down, the larger grains being of 30µm. Then the powder was mixed with epoxy resin and subsequently aligned at room temperature using an orientation field of typically 1T. The magnetic measurements were performed using an automatic system [18] equipped with a cryostat associated with a calorimeter. The saturation magnetization has been obtained from extrapolation of the M(H) curve with H parallel to the alignment direction.

Neutron diffraction experiments were carried out at the high flux reactor of the Institut Laue Langevin. The two axes D1B powder diffractometer used for this work was equipped with a large one dimensional 400 cell curved detector which recorded the diffraction pattern over a 2Θ range of 80°. The neutron wavelength of 1.28 Å was

selected by the (311) reflection of a germanium monochromator and the 2Θ step was 0.2°.

High resolution powder diffraction patterns have been collected on the D1A spectrometer and neutrons with a wavelength of 3.111 and 2.579 Å for the acquisition at 2 and 295 K respectively. The data were collected for ca. 12 hours over a 2Θ range of 5 to 155° with a step of 0.05° on fine powder placed in a thin-walled vanadium container. All powder neutron diffraction data were analyzed using the Rietveld line profile technique implemented with the program FULLPROF [19].

3. Structural results

The insertion of hydrogen within the lattice has led to about one H atom per formula unit of $RFe_{12-x}Ti_x$. As can be seen from Fig. 1, this has induced an increase of the unit cell volume which mostly originates from the increase of the c lattice parameter. The increase of the lattice parameter is moderate and is about 1% (c.a. 1.5$Å^3$ /H atom) whatever the rare-earth element alloyed. This magnitude of the unit cell expansion is in agreement with other studies [5,20]. The unit cell increase is anisotropic even if both lattice parameters expand. It is worth to mention that whereas the c lattice parameter is almost constant along the $RFe_{12-x}Ti_x$ series, in the corresponding hydrides there is a continuous decrease of the c lattice parameter reflecting the lanthanide contraction (Fig. 1). This indicates that whereas the c lattice parameter was mostly determined by the Fe(Ti)-Fe(Ti) inter-atomic distances in the starting compounds, in the corresponding hydrides the size of the rare earth plays a major role.

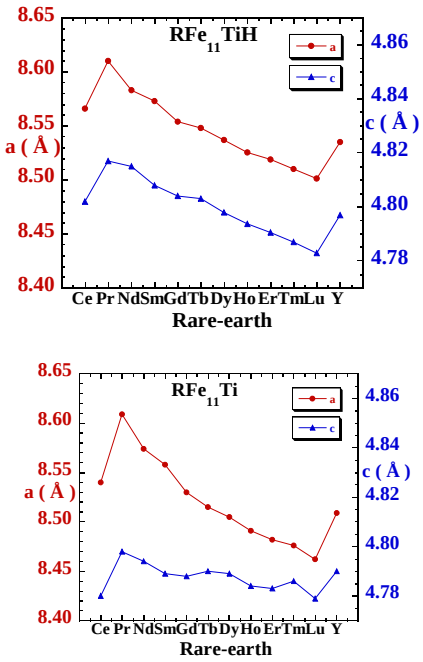

Fig. 1. Evolution of the lattice parameters of the $RFe_{11}Ti$ and $RFe_{11}TiH$ compounds along the rare-earth series.

Indeed, according to the analysis of the neutron diffraction patterns recorded for $TmFe_{11}TiH$ and $TbFe_{11}TiH$, the H insertion occurs in the rare-earth environment in a pseudo octahedral site as shown in Fig. 2 and 4 respectively. The corresponding 2b position is presented in the crystal structure of Fig. 3, and the results of the Rietveld refinements are given in Tables 1 and 2 for the $TmFe_{11}Ti$ and $TbFe_{11}TiH$ compounds respectively. The rare-earth dependence of the c lattice parameter reflects the sequence R-H-R along the c axis which is at the origin of the increase of the c lattice parameter upon hydrogen insertion. At 300 K, the interatomic distances between H and its neighbors are the following d_{Tb-H}=2.40Å and d_{Fe-H}=1.92Å.

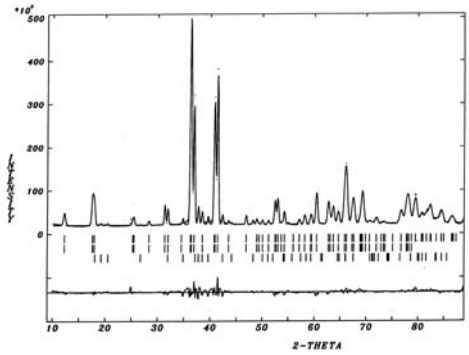

Fig. 2. The powder neutron diffraction pattern of $TmFe_{11}TiH$ obtained at 300 K on the D1B diffractometer. The points represent the experimental data and the solid line is the result of the Rietveld profile analysis. The difference between the experimental data and the calculated pattern is plotted on the same scale in the lowest part of the figure. In between, the first and second rows of vertical lines refer to the $TmFe_{11}TiH$ nuclear and magnetic contributions to the diffraction pattern respectively. The third rows refer to the contributions of $TiFe_2$ to the diffraction pattern. The wavelength used is equal to 1.287 Å.

In the $TmFe_{11}TiH$ compounds the corresponding distances are shorter: d_{Tm-H}=2.39 Å, and d_{Fe-H}=1.89 Å in agreement with the smaller size of Tm comparison with Tb leading to a smaller unit cell. The occupancy of the interstitial site by hydrogen is close to 100% Tables 1 and 2. This confirms the amount of one H atom per formula unit estimated from the synthesis. Traces of $TiFe_2$ as impurity have been observed by neutron diffraction in both compounds, impurity that was not detectable by X-ray diffraction. As can be seen from the Tables 1 and 2, the magnetic moment refined at low temperature on the Fe atoms are slightly larger than the one usually reported for the $RFe_{12-x}Ti_x$, indicating that the hydrogen insertion induces the increase of the Fe magnetic moments. This has been described to the overall increase of the Fe-Fe exchange interactions due to the increase of the overall Fe-Fe interatomic distances. Another result of the neutron diffraction is the location of the Ti atom on the 8i position, this is clearly related to the larger size of this crystal site in comparison with the two other 8j, 8f sites [15,17,21].

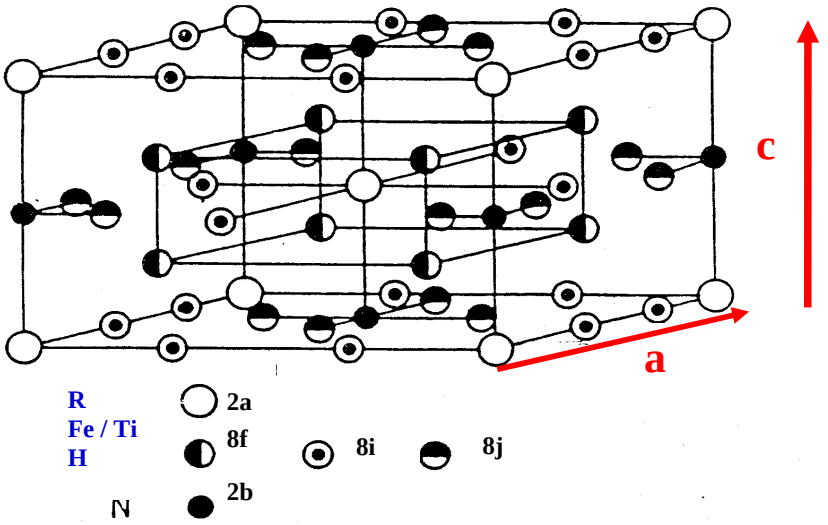

Fig. 3. Schematic representation of the crystal structure of the $RFe_{11}TiH$ compounds.

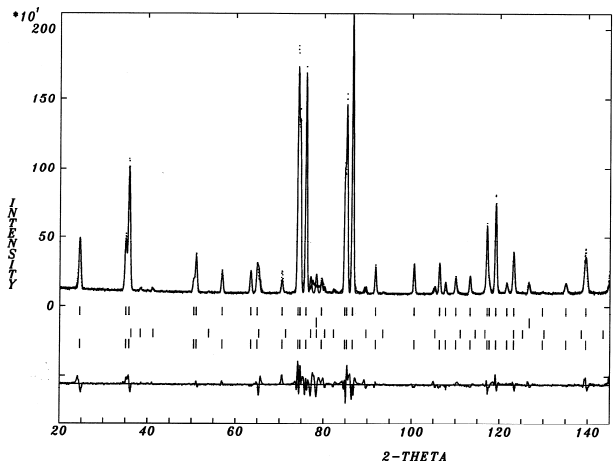

Fig. 4. The powder neutron diffraction pattern of $TbFe_{11}TiH$ obtained at 300 K on the D1A diffractometer. The points and the solid line represent the experimental data and the Rietveld profile analysis respectively. The difference between the experimental data and the calculated pattern is plotted on the same scale in the lowest part of the figure. In between, the first and fourth rows o f vertical lines refer to the $TbFe_{11}TiH$ nuclear and magnetic contributions to the diffraction pattern respectively. The second and third rows refer to the contributions of Fe and $TiFe_2$ to the diffraction pattern. The wavelength was 2.579 Å.

Table 1. The positional parameters, isotropic thermal factors, and moments in $TmFe_{11}TiH$ at 300 K. The agreement factors were as follows Rp=6.14 %; R_B=6.77% ; R_{Mag}=9.3 %.

Atom	site	x	y	z	B (Å^2)	Occ. (%)	M (μ_B)
Tm	2a	0	0	0	0.5	100	-1.6 (0.3)
Fe	8f	0.25	0.25	0.25	0.6	100	2.1 (0.2)
Fe	8j	0.2775(4)	0.5	0	0.6	100	2.2 (0.2)
Fe / Ti	8i	0.3527(5)	0	0	0.6	77/ 23 (1)	2.5 (0.2)
H	2b	0	0	0.5	2.2	93 (3)	-

Table 2. The positional parameters, isotropic thermal factors, and moments in $TbFe_{11}TiH$ at 2 and 300 K. The agreement factors were as follows at 2K : R_p=7.68 %; R_B=4.0% ; R_{Mag}=5.67% and at 300K : R_p=6.28%; R_B= 4.6% R_{Mag}= 9.2%.

Atom	site	x	y	z	B ($Å^2$)	Occ. (%)	M (μ_B) @ 2 / 300 K
Tb	2a	0	0	0	0.5	100	-8.0 / -6.0(0.1)
Fe	8f	0.25	0.25	0.25	0.5	100	2.2 / 1.9(0.1)
Fe	8j	0.2760(5)	0.5	0	0.5	100	2.2 / 1.9 (0.1)
Fe / Ti	8i	0.3581(7)	0	0	0.5	76/24 (2)	2.2/ 1.9 (0.1)
H	2b	0	0	0.5	2.0	92 (3)	-

4. Magnetic measurements

The isothermal magnetic measurements reported in Fig. 5 are given at 4 and 300 K for both $TmFe_{11}Ti$ and $TmFe_{11}TiH$. In both cases the magnetization results from the difference between the antiferromagnetically coupled Tm and Fe sublattice. At the room temperature, magnetization is larger than at 4 K because of the fast decrease of the Tm magnetization. Whereas at 300 K the hydride exhibits a larger magnetization than $TmFe_{11}Ti$, at 4 K both magnetization curves are very similar meaning that this is mostly the temperature dependence of the magnetization that is modified upon hydrogen insertion. This is in close agreement with the large increase of the ordering temperature of the $RFe_{11}Ti$ [5] and the moderate magnetization increase that have been observed [5,6,15,22] upon hydrogenation. In the case of the Tm compounds, the Curie temperature has been measured at 500 (±5) and 529 (±5)K for $TmFe_{11}Ti$ and the corresponding hydride respectively. As can be seen from Fig. 5 the saturation of the Tm compounds is rather difficult to achieve because of the huge uniaxial magnetocrystalline known to result from the addition of the Fe and Tm sublattice anisotropy of these compounds [3,4,13,14]. On the contrary $TbFe_{11}Ti$ has been reported to present a spin reorientation slightly above room temperature resulting from the competition of the magnetocrystalline anisotropy of Tb and of the Fe atoms. As a consequence the saturation of the $TbFe_{11}TiH_x$ compounds is easily obtained in the high magnetic field used in Figure 6. Furthermore, due to the proximity to this spin reorientation temperature, the $TbFe_{11}Ti$ compound presents a very small magnetocrystalline anisotropy as can be seen from Fig. 6. In the case of the $TbFe_{11}TiH$ phase the magnetic anisotropy is much larger and the field at which the curves recorded when applying the field perpendicular to the orientation direction merges the curves recorded when applying the field parallel to the orientation direction is about 10KOe. It has been shown that $TbFe_{11}TiH$ presents a basal plane magnetocrystalline anisotropy up to its Curie temperature following the dominant Tb magnetocrystalline anisotropy [5,13,14,23,24]. Our present investigation shows that in spite of the competition between the Tb and Fe sublattice anisotropy, at room temperature this compound keep a large anisotropy field. Indeed a value of c.a. 15T is measured for $TbFe_{11}TiH$. The anisotropy field of $TbFe_{11}TiH$ is even larger at low temperature and a value of more than 22T is obtained at 4.2 K. This clearly reflects the hydrogen induced reinforcement of the magnetocrystalline anisotropy of the rare-earth sublattice. This behaviour has been explained by the increase of the crystal electric field gradient experienced at the rare-earth site [10], a phenomenon occurring upon hydrogen insertion in the rare-earth environment. To our knowledge no work has been devoted to the physical properties of the $TmFe_{11}TiH_x$ compounds. Our study shows that no spin reorientation like phenomenon can be detected by ac susceptibility at low temperature and no anomaly has been observed above room temperature either. This indicates that the easy magnetization axis remains the same up to the Curie temperature for both $TmFe_{11}Ti$ and its corresponding hydride. This is not surprising since in $TmFe_{11}Ti$ both Tm and Fe sublattice are known to prefer orientation of their magnetic moment along the c axis of the structure. As previously discussed the insertion of hydrogen in the rare-earth neighborhood induces an increase of the rare-earth contribution to the magnetocrystalline anisotropy. One can thus expect an even larger uniaxial character for the $TmFe_{11}TiH$ compound. Consequently no spin reorientation can be expected for the $TmFe_{11}TiH$ compound since the two different magnetic sublattices (Tm and Fe one) favor the same easy axis direction : the c axis.

In $TbFe_{11}TiH$, the Mössbauer spectroscopy investigation has shown that the alignment of the Fe magnetic moment is along the basal plane of the structure [23] between 4.2 and 300 K. No anomaly of the ac susceptibility has been observed above room temperature up to the Curie temperature which indicates that this basal plane anisotropy is kept up to the Curie temperature [5]. This is in excellent agreement with the result reported earlier for $TbFe_{11}TiH$ [24]. Using single crystal they have shown that the easy magnetization direction is along the [110] direction at 4.2 K. According to the present neutron diffraction analysis, the Tb magnetic moment obtained at low temperature is large: $8\mu_B$ and remains rather large even at room temperature: 6 μ_B. This reflects the rather high ordering temperature of the $TbFe_{11}TiH$ compound. Indeed the Curie temperature of $TbFe_{11}Ti$ and $TbFe_{11}TiH$ are 578 and 620 (±5) K, respectively [5,23]. As expected due to the smaller magnetic moment magnitude of the free ion value, in $TmFe_{11}TiH$, the Tm atom exhibits a much smaller magnetic moment at room temperature 1.6 μ_B.

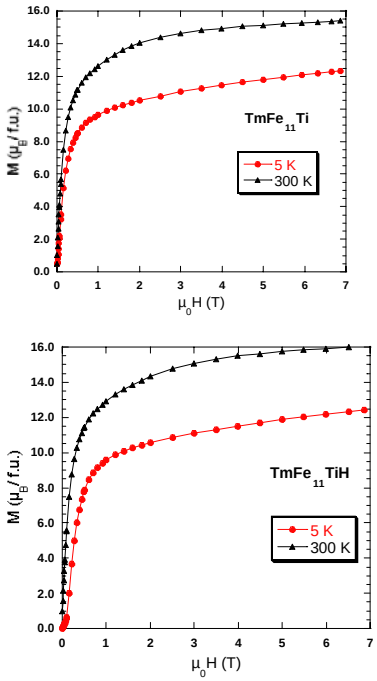

Fig. 5. Isothermal magnetization curves recorded at the indicated temperatures for $TmFe_{11}Ti$ and $TmFe_{11}TiH$ on powder samples.

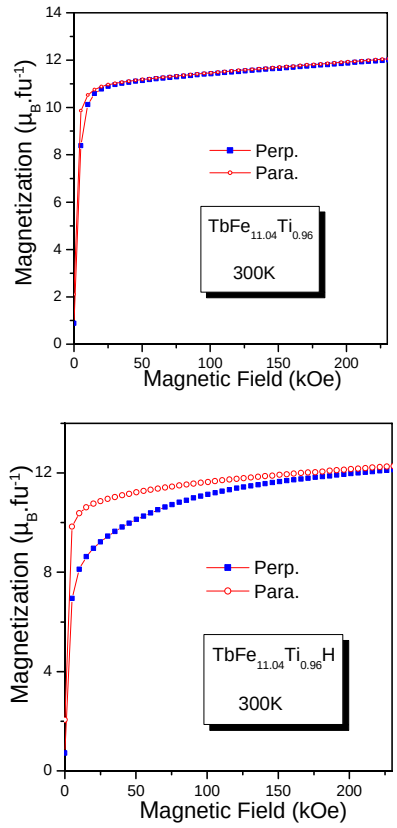

Fig. 6. Isothermal magnetization curves at 300 K recorded $TbFe_{11}Ti$ and its hydride, the field being either parallel or perpendicular to the alignment direction (alignment performed at 300K).

The obtained magnetic moment on the Fe sites are about 2 μ_B/Fe atom, a value which is in reasonable agreement with estimation from the saturation magnetization of isotype $YFe_{11}TiH$ or $LuFe_{11}TiH$ compounds [20,25]. We have seen in the previous section that hydrogen insertion induces an expansion of the crystal lattice. This can be described as being equivalent to a negative pressure effect acting on the lattice [5]. Such analogy can be also useful to analyse the effect of hydrogen on the magnetic properties: in the $RFe_{11}Ti$ compounds (R=Lu, Y) both the Curie temperature and the iron sublattice magnetization have been shown to decrease upon applying an external pressure [7,8]. The present neutron diffraction investigation shows that the iron magnetic moments are large in the hydride confirming earlier published results obtained by magnetic measurements [6,22,25,26] or Fe Mössbauer spectroscopy [13,14,26]. The effect of H on the Fe sublattice magnetization is thus opposite to that of an applied pressure and was estimated to be equivalent to a negative pressure of -23kbar per inserted H atom.

Finally, it is interesting to note that not all the magnetic properties are completely changed upon hydrogenation, indeed it has been recently shown that unlike the magnetization and the ordering temperature which are increased, the rare-earth-iron exchange coupling remains unchanged after hydrogen insertion [27].

5. Conclusions

Insertion of hydrogen atom has been performed in the $RFe_{11}TiH$ compounds leading to an anisotropic unit cell expansion. A maximum of 1 H atom per formula unit has been accommodated within the crystal structure. Powder neutron diffraction has been use to locate the hydrogen atom in the pseudo octahedral interstitial site of the crystal structure of $TmFe_{11}TiH$ and $TbFe_{11}TiH$. This insertion occurs in the rare-earth environment, hydrogen becoming the first near neighbor of the rare-earth atoms. In spite of the moderate lattice expansion occurring upon hydrogen insertion in the $RFe_{11}Ti$ compounds, the effect of hydrogen on the magnetic properties is dramatic. In addition to the increase of both the Curie temperature and the magnetization, modification of the magnetic phase diagram can be observed. The insertion of hydrogen reinforces the basal magnetic anisotropy of the terbium sublattice and the spin reorientation observed in $TbFe_{11}Ti$ at 338K disappears in $TbFe_{11}TiH$. The magnetocrystalline anisotropy of the hydride is large even at room temperature. For $TmFe_{11}Ti$ the insertion of hydrogen within the lattice does not change the easy magnetization direction but induces an increase of the Curie temperature and of the magnetization.

References

[1] D. B. de Mooij, K. H. J. Buschow, J. Less Common Met. **136,** 207 (1988).
[2] K. H. J. Buschow J. Magn. Magn. Mater. **100,** 79 (1991).

[3] B. P. Hu, H. S. Li, J. P. Gavigan, J. M. D. Coey, J. Phys.: Condens. Matter **1,** 755 (1989).
[4] X. C. Kou, Zhao T. S, Grössinger, R. Kirchmayer, H. R. Li, X and de Boer F.R. Phys. Rev. B **47,** 3231 (1993).
[5] O. Isnard J. Alloys Compounds **356/357,** 17 (2003).
[6] O. Isnard, M. Guillot, S. Miraglia, D. Fruchart J. Appl. Phys. **79,** 5542 (1996).
[7] J. Kamarad, S. A. Nikitin, Z. Arnold, I. S. Tereshina, High Pressure Research **161-164**, 23 (2003).
[8] Z. Arnold, J. Kamarad, O. Mikulina, B. Garcia-Landa, C. Abadia, M. R. Ibarra, N. V. Kudrevatykh, J. Magn. Magn. Mater. **196-197,** 748 (1999).
[9] M. D. Kuzmin, A. K. Zvezdin, J. Appl. Phys. **83**, 3239 (1998).
[10] O. Isnard, P. Vulliet, J.P. Sanchez, D. Fruchart, J. Magn. Magn. Mater. **189,** 47 (1998).
[11] D. P. F. Hurley J. M. D Coey J. Phys. Cond. Matter **4,** 5573 (1992).
[12] Qi-Nian Qi, Y. P. Li, J. M. D. Coey, J. Phys. Cond. Matter. **4**, 8209-8220 (1992).
[13] C. Piquer, F. Grandjean, O. Isnard, G. J. Long, J. Phys. Condens. Matter. **18**, 205 (2006).
[14] C. Piquer, F. Grandjean, O. Isnard, G.J. Long J. Phys. Condens. Matter. **18**, 221 (2006).
[15] O. Isnard, S. Miraglia, M. Guillot D. Fruchart J. Alloys Compounds **275–277**, 637 (1998).
[16] Ph. Oleinek, O. Isnard, P. Convert, K. H. Müller, M. Loewenhaupt, L. Schultz, J. Alloys and Comp. **298**, 220 (2000).
[17] A. Apostolov, R. Bezdushnyi, N. Stanev, R. Damianova, D. Fruchart, J. L. Soubeyroux, O. Isnard, J. Alloys and Comp. **265**, 1 (1998).
[18] J. C. Picoche, M. Guillot, A. Marchand, Physica B **155,** 407 (1989).
[19] J. Rodriguez-Carvajal, Physica B **192,** 55 (1993).
[20] N. S. Nikitin, I. S. Tereshina, V. N. Verbetsky, A. A. Salamova, J. Alloys and Compds. **316**, 46 (2001).
[21] O. Isnard, D. Fruchart, J. Alloys and Comp. **205**, 1 (1994).
[22] O. Isnard, M. Guillot, J. Applied Phys. **83,** 6730 (1998).
[23] C. Piquer, R. P. Hermann, F. Grandjean, O. Isnard, G. J. Long J. Phys. Condens. Matter **15**, 7395-7409 (2003).
[24] N. S. Nikitin, I. S. Tereshina, V. N. Verbetsky, A. A. Salamova, K. P. Skokov, N. Yu. Pankratov, Yu. V. Skourski, N. V. Tristan, V. V. Zubenko, I. V. Telegina, J. Alloys and Compds. **322,** 42 (2001).
[25] C. Piquer, F. Grandjean, G. J. Long, O. Isnard, J. Alloys and Comp. **383**, 6 (2005).
[26] I. S. Tereshina, P. Gaczynski, V. S. Rusakov, H. Drulis, S. A. Nikitin, W. Suski, N. V. Tristan, T. Palwski, J. Phys.: Condens. Matter. **13**, 8161 (2001).
[27] O. Isnard, M. Loewenhaupt, R. Bewley, Physica B **350** suppl. 1 e31, (2004).

*Corresponding author: olivier.isnard@grenoble.cnrs.fr